J Mater Sci (2009) 44:5249–5255
DOI 10.1007/s10853-009-3465-0

FERROELECTRICS

Ab initio study of antiferroelectric $PbZrO_3$ (001) surfaces

G. Pilania · D. Q. Tan · Y. Cao · V. S. Venkataramani · Q. Chen · R. Ramprasad

Received: 25 March 2009 / Accepted: 3 April 2009 / Published online: 17 April 2009

Abstract We have carried out first-principles total-energy calculations of bulk and (001) surfaces of $PbZrO_3$. The ground state for bulk $PbZrO_3$ is determined to be the antiferroelectric orthorhombic phase, with the ferroelectric rhombohedral and paraelectric cubic phases being 0.14 and 0.39 eV per formula unit higher in energy, respectively. PbO- and ZrO_2-terminated (001) surfaces, either clean or when hydroxyl species were adsorbed were considered. Surface relaxations, in-plane antiferroelectric distortions and modifications to the electronic structure due to the surfaces, and hydroxyl adsorbates on the surfaces were investigated. We find that while clean surfaces retained bulk-like behavior, hydroxyl adsorbates induce significant changes to the surface geometry as well as introduce electronic states in the band gap possibly rendering the surfaces metallic.

Introduction

Perovskite oxides of ABO_3 type constitute an important class of materials which display a wide variety of electronic properties, complex structural instabilities, and play an important role in numerous electronic, optical, and chemical applications [1–5]. Lead zirconate, $PbZrO_3$ (PZ), is a distinguished member of this class of materials. Pure PZ is known to exhibit three different phases: a low temperature orthorhombic antiferroelectric phase (A_O) stable up to 230 °C, a rhombohedral ferroelectric phase (F_R) stable at 230–233 °C, and a cubic paraelectric phase (P_C) above 233 °C. Apart from being a simple antiferroelectric prototype, PZ is the extreme end point of the industrially important solid–solution $Pb(Zr,Ti)O_3$ (PZT).

The earliest reported structure [6] and subsequent refinement of bulk antiferroelectric PZ were based on a combination of X-ray diffraction and neutron diffraction experiments [7–14], and density functional theory (DFT) based calculations [15, 16]. The structure of the higher energy P_C phase has also been studied experimentally (see Ref. [17], and references therein), and point defects (F-centers) in this phase have been characterized computationally as well [18].

Although detailed studies of the surfaces of various perovskites such as $BaTiO_3$, $PbTiO_3$, $SrTiO_3$, etc., have been performed, such studies of an antiferroelectric system such as PZ has not been reported to date. In this paper, we take initial steps toward filling this gap through a study of the PbO- and ZrO_2-terminated (001) surfaces, both when they are clean and when they possess excess oxygen (e.g., when the surfaces are "capped" with hydroxyl species). Modifications of the electronic structure and antiferroelectric distortions (relative to the equilibrium bulk) due to the surfaces and surface hydroxyl species have been extensively investigated. We find that these properties are extremely sensitive to the details of the surface structure.

The remainder of this paper is organized as follows. In section "Methodology details", we provide details concerning the computational methodology used. Our results

G. Pilania · R. Ramprasad (✉)
Chemical, Materials, and Biomolecular Engineering, Institute of Materials Science, University of Connecticut, Storrs, CT 06269, USA
e-mail: rampi@ims.uconn.edu

G. Pilania
e-mail: gpilania@gmail.com

D. Q. Tan · Y. Cao · V. S. Venkataramani · Q. Chen
GE Global Research Center, One Research Circle, Niskayuna, NY 12309, USA

for all three bulk phases of PZ are discussed in section "Bulk $PbZrO_3$ phases", followed by a description of the clean (001) surface results in section "Clean (001) surfaces". The impact of hydroxyl adsorption on the clean surfaces are discussed in section "Hydroxyl-covered (001) surfaces". Finally, our conclusions are summarized in the final section.

Methodology details

Our calculations were carried out using DFT as implemented in the VASP code [19] with the electronic wave functions expanded in a plane wave basis with a cutoff energy of 400 eV. The generalized gradient approximation (GGA) with projector augmented wave (PAW) method was used. The atomic positions were relaxed until the maximum component of the force on any atom was smaller than 0.02 eV/Å. Calculations were done using a (4,4,4) Monkhorst-Pack mesh [20] for the bulk P_C and F_R phases. The bulk A_O phase and the corresponding slab surface calculations employed Monkhorst-Pack meshes of (4,4,2) and (4,4,1), respectively, to produce converged results.

Results

Bulk $PbZrO_3$ phases

The calculated lattice parameter of the P_C phase (in space group $Pm\bar{3}m$) was found to be 4.158 Å in good agreement with previous theoretical (4.177 Å) [18] and experimental (4.161 Å at 520 K) [21] results. The F_R phase (in space group R3m) is specified by a lattice parameter and the three internal parameters δ_{Zr}, δ_{O1}, and δ_{O2} (representing the ferroelectric displacements of the Zr and O atoms [22]). The computed lattice parameter and the internal parameters δ_{Zr}, δ_{O1}, and δ_{O2} for the F_R phase were 4.176 Å, 0.446 Å, 0.014 Å, and 0.041 Å, respectively, in good agreement with prior DFT work [22].

Table 1 shows the computed fractional coordinates of all symmetry unique atoms and the lattice parameters of PZ in the A_O phase, along with low temperature experimental data. As can be seen, the calculated results are in excellent agreement with experiments. The center panel of Fig. 1 shows top and side views of the A_O unit cell, in which the ZrO_6 octahedra can be seen to be distorted and tilted in an alternating manner. We mention that the P_C phase is characterized by regular, untilted, ZrO_6 octahedra. The tilting and the distortion of the octahedra in the A_O phase causes displacements of the atoms from their corresponding P_C positions. The left panel of Fig. 1 shows the antiferroelectric nature of the displacements of the atoms in (001) planes which are composed of either PbO or ZrO_2 layers arranged alternately. Inspection of the displacements indicates that there is no net in-plane dipole moment in any (001) plane. Successive PbO layers show displacement of O atoms along opposite directions, with non-negligible movements of Pb atoms. In contrast, atomic displacements are identical in successive ZrO_2 layers, with Zr atoms undergoing negligible displacements. The right panel of Fig. 1 shows the layer-decomposed density of states (LaDOS) for the PbO and ZrO_2 (001) layers, determined by decomposing the total density of states (DOS) in terms of contributions made by each layer of atoms. Based on these results we report a band gap value of 3.15 eV for the bulk A_O phase, in good agreement with prior DFT work [23].

Table 1 Fractional coordinates of atoms and lattice parameters for the A_O phase of $PbZrO_3$ calculated in the present study compared with experimental results

		This study			Experimental (10 K)		
		x	*y*	*z*	*x*	*y*	*z*
Fractional coordinates	Pb1	0.707	0.122	0	0.699	0.123	0
	Pb2	0.714	0.128	0.5	0.706	0.129	0.5
	Zr	0.244	0.125	0.25	0.241	0.125	0.249
	O1	0.277	0.162	0	0.276	0.156	0
	O1′	0.3	0.09	0.5	0.301	0.096	0.5
	O2	0.032	0.262	0.285	0.032	0.262	0.28
	O3	0	0.5	0.199	0	0.5	0.203
	O4	0	0	0.222	0	0	0.23
Lattice parameters (Å)	a		5.876			5.874	
	b		11.814			11.777	
	c		8.217			8.191	

Notation of the atom sites are same as adopted in Ref. [14]

Our calculations show that the A_O phase is the ground state, with the F_R and P_C phases being 0.14 and 0.39 eV higher in energy per $PbZrO_3$ formula unit, respectively. These determinations are in good agreement with prior work; Leung and Wright [24] report a value of 0.37 eV as the energy difference between the P_C and A_O phases, and Singh [15] obtains 0.25 eV as the energy difference between the P_C and F_R phases (identical with our determination).

Clean (001) surfaces

Next, we turn our attention to clean (001) surfaces modeled using slabs terminated symmetrically on both sides with either PbO or ZrO_2 surfaces. The central panels of Figs. 2 and 3 show top and side views of the slab supercell geometry. A 12 Å vacuum region was used between slabs,

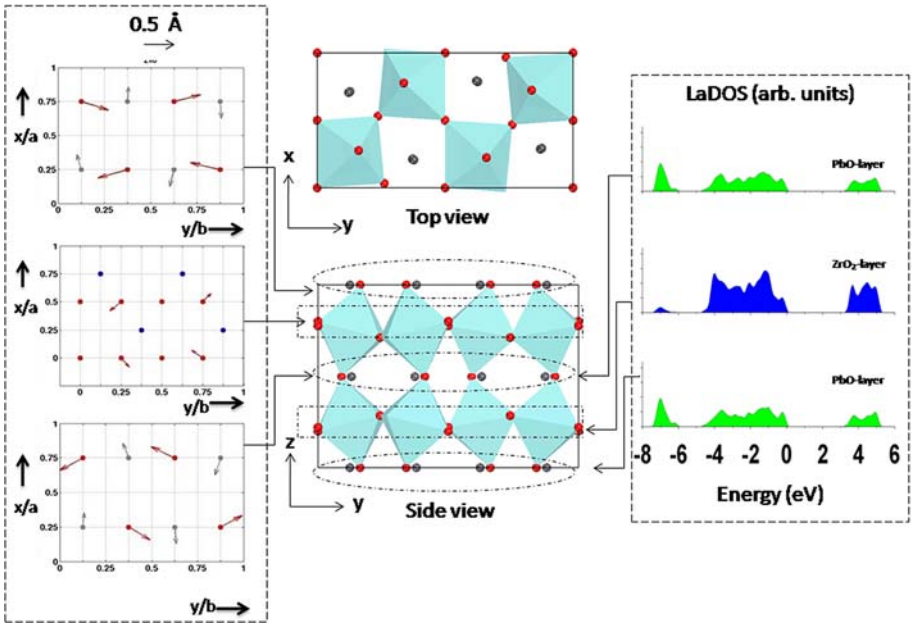

Fig. 1 *Center panel* Top and side views of the relaxed A_O unit cell. *Left panel* Atomic displacements of atoms with respect to the atomic positions in pseudo-cubic phase (cubic phase strained to match with orthorhombic unit cell) along the (001) planes. *Right panel* Layer-decomposed density of states (LaDOS) for the (001) planes; the zero of the energy coincides with the valence band maximum. Note that the (001) planes are composed of PbO and ZrO_2 layers arranged alternately. Pb, Zr, and O atoms colored *gray*, *blue*, and *red*, respectively. Zr atoms (not explicitly shown in the center panels) are at the center of the (ZrO_6) octahedra. The atomic displacements and LaDOS are shown only for symmetry unique (001) planes

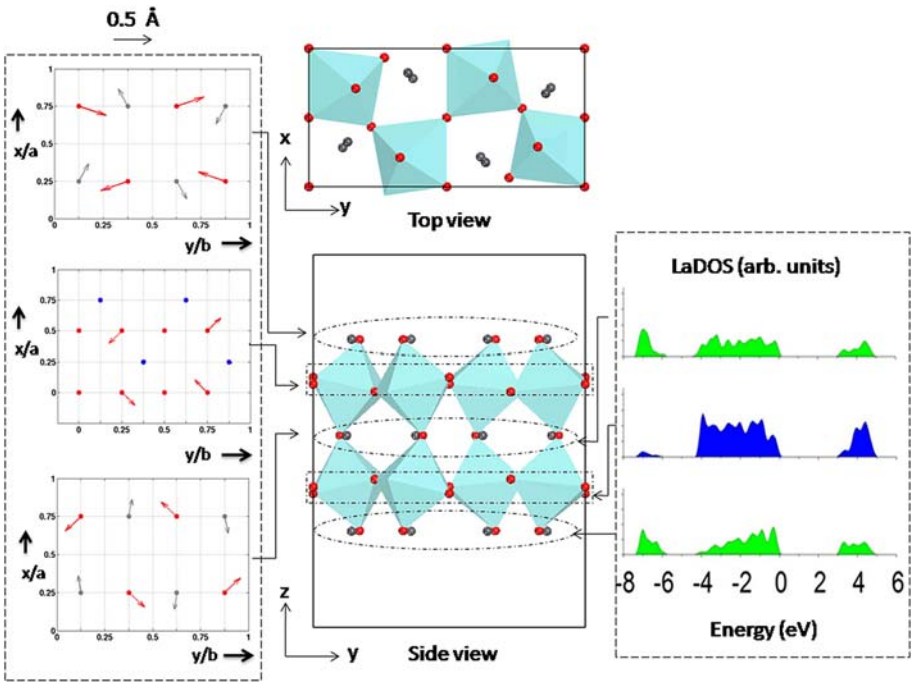

Fig. 2 Same as Fig. 1, but for the clean PbO-terminated (001) slab

normal to the surface plane, to minimize spurious interactions between a slab and its adjacent periodic image (along the [001] direction). The clean PbO-terminated slab contained five alternating PbO and ZrO_2 (001) layers (with the central PbO layer constituting a mirror plane), while the clean ZrO_2-terminated slab contained seven alternating PbO and ZrO_2 layers (again, with the central PbO layer serving as a mirror plane). The clean PbO and ZrO_2-terminated slabs thus contained 48 and 72 atoms per supercell, respectively.

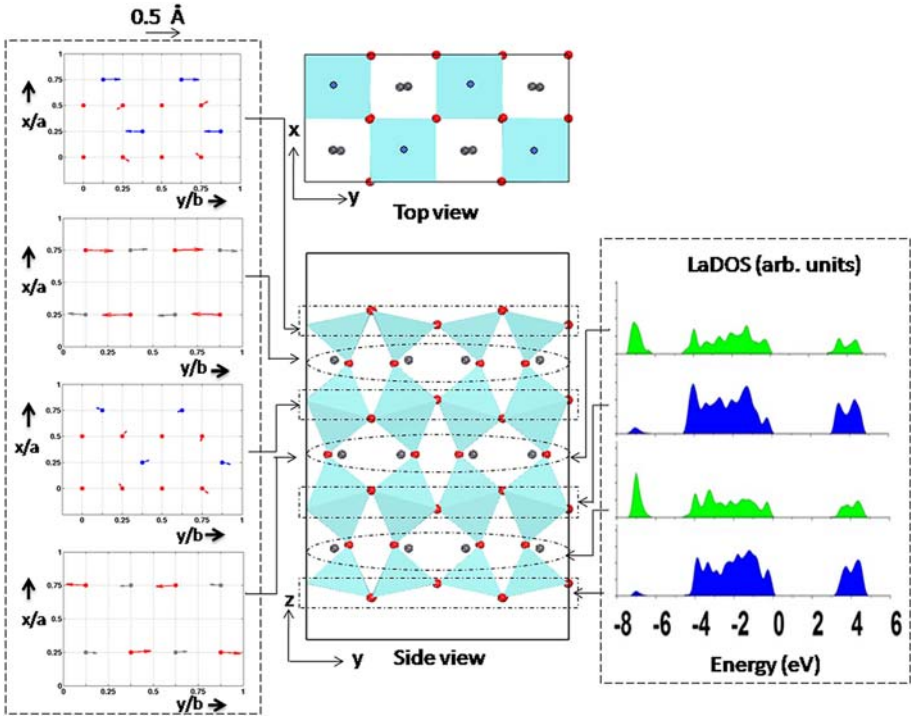

Fig. 3 Same as Fig. 1, but for the clean ZrO_2-terminated (001) slab

We first consider the clean PbO-terminated slab (Fig. 2). After relaxation, the surface (PbO layer) and near-surface (ZrO_2 layer) planes display in-plane atomic displacements almost identical to that in the bulk (cf. Fig. 1). Consistent with this trend, the surface relaxations displayed by this slab are small, as can be seen from Table 2 (−1.6% for the top-most two layers, and +2.9 % for the next two layers). We note that unlike in the bulk phase where all Pb and O atoms in a PbO layer lie in the same plane, the surface PbO layer in the PbO-terminated slab contains a non-zero surface rumpling. All O atoms in the surface PbO layer are displaced by 0.021 Å inward below the Pb atomic plane. This behavior is in contrast with other ABO_3 perovskites (such as $PbTiO_3$ or $BaTiO_3$), where the metallic atoms in the outer AO layer move inward while the surface O atoms move out of the slab to produce a surface rumpling [25].

In Fig. 2 we also report the LaDOS for each layer in the slab, which are similar to the bulk, reported in Fig. 1. We do not find any mid gap surface states in the band gap, although the band gap has slightly decreased (to 2.95 eV) from its bulk value.

Next, we turn our discussion toward the ZrO_2-terminated clean surface (Fig. 3). A striking difference is evident on comparing the in-plane atomic displacements of the various layers in this slab (left panel of Fig. 3) with the corresponding bulk displacements. Unlike the negligible Zr atomic displacements in bulk and clean PbO-terminated slabs, large in-plane displacements of Zr atoms can be seen in the surface layer. However, the Zr atoms still maintain the net zero in-plane dipole moment (note the antisymmetric nature of the displacements), while O atom displacements still follow the bulk-like pattern with somewhat decreased magnitude. Polarization induced by the large antiparallel displacements of Zr atoms does not remain confined only in the outer surface layer but propagates inward. As a result, the penultimate PbO layer also bears strong polarizations. It can be clearly seen from Fig. 3 that all Pb and O atoms get displaced commensurate with Zr displacements. As we move inward, Zr atomic displacements get reduced as compared to the surface layer and approach bulk-like behavior as one might expect, but displacements of Pb and O atoms in PbO layers have a relatively slow convergence toward bulk behavior. The above results show the extreme sensitivity of polarization distortions on the nature of the surface. The percentage interlayer relaxations, reported in Table 2, follow the expected trend of decay as we go inward. However the percentage reduction in the distance

Table 2 Percentage change in the interlayer spacing d_{ij} relative to the corresponding bulk layer spacing

Termination	Type	Δd_{12}	Δd_{23}	Δd_{34}
PbO	Clean	−1.6	2.9	–
ZrO_2	Clean	−12.0	9.8	0.0
PbO	–OH adsorbed	45.8	16.1	–
ZrO_2	–OH adsorbed	−0.4	10.4	2.0

The interlayer distances are based on the positions of the relaxed metal ions

between the pair of outermost layers is significantly large (−12.0 %) compared to −1.6 % in case of the PbO-terminated slab. This relaxation is mainly because of the large outward movement of Pb atoms in the near-surface PbO layer, which also results in a large surface rumpling of 0.16 Å in this layer. The LaDOS results shown in Fig. 3 for ZrO_2-terminated clean slab are qualitatively similar to that of the PbO-terminated clean slab with no surface states evident in the band gap. The band gap value was also found to be the same as that calculated for the PbO-terminated slab.

Hydroxyl-covered (001) surfaces

The hydroxyl-covered (001) slabs were modeled by placing a –OH species on top of each metal atom of the clean PbO and ZrO_2-terminated slabs, followed by optimization of the geometry. These slabs are intended to model oxidized surfaces containing a higher concentration of surface oxygen than allowed by the metal oxide stoichiometry. The central panels of Figs. 4 and 5 portray the top and side views of the hydroxyl-adsorbed PbO- and ZrO_2-terminated slabs, respectively.

Focusing first on the PbO-terminated case, we note that the in-plane displacements of atoms (left panel of Fig. 4) are qualitatively similar to those plotted for the clean PbO-terminated slab in Fig. 2, but the out of plane displacements in the two slabs differ significantly. Huge outward displacements of surface Pb atoms in the outer layer can be seen from the side view of the relaxed geometry in Fig. 4. This leads to a surprisingly large inter layer relaxation of 45.75 % for the outer most layers for this slab (Table 2). The hydroxyl species relax to bridge positions between adjacent Pb atoms.

Moving on to the hydroxyl-adsorbed ZrO_2-terminated slab, it can be seen (from its relaxed geometry shown in Fig. 5) that the O atom of the hydroxy group relaxes to a position such that it completes the ZrO_6 octahedron. The hydroxyl layer thus plays the role of a PbO layer with the Pb atoms missing and the O atoms passivated with H. Consistent with this observation, the in-plane atomic displacements (left panel of Fig. 5) for this slab are qualitatively similar to that in the bulk, and the inter-layer relaxations for the topmost two layers are small while that for the next two layers are large (presumably due to the absence of Pb atoms in the topmost layer). The relaxations reach small values subsequently, indicating that a bulk-like environment is gradually restored (Table 2).

Finally, we comment about the changes in the electronic structure due to hydroxyl adsorption. The right panels of Figs. 4 and 5 display the LaDOS for the PbO- and ZrO_2-terminated cases. It can be seen that hydroxyl adsorption introduces states in the band gap for both surface terminations. The surface states persist deeper into the interior of the slab in the case of the PbO-terminated slab indicating the sensitivity of the electronic structure to the surface preparation. In essence, we conclude that the presence of hydroxyl species on PZ (001) surfaces could lead to metallic behavior in the near-surface region. Still, the quick restoration of bulk-like behavior in the slab interior regions

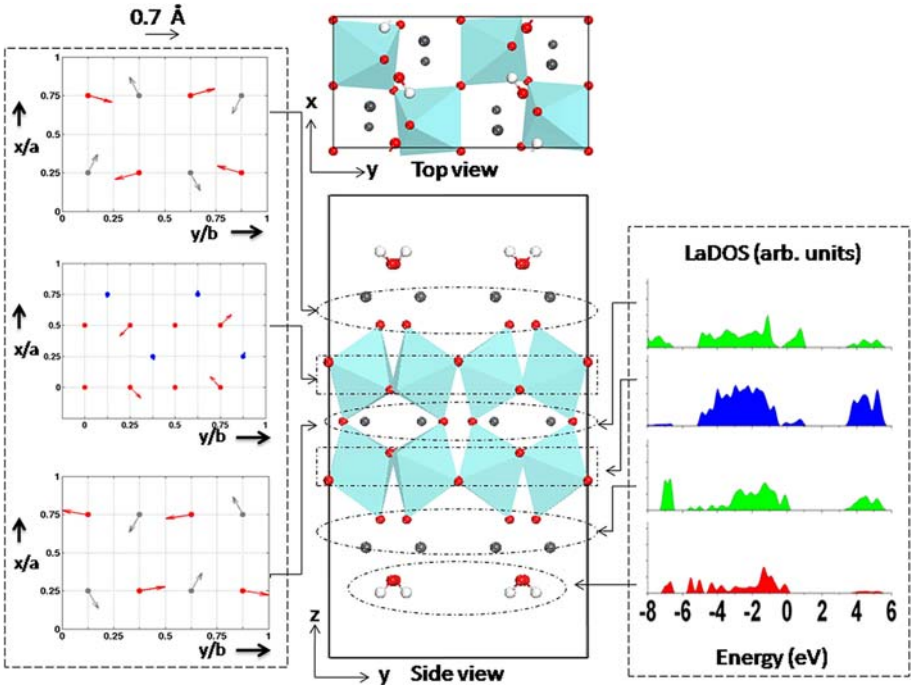

Fig. 4 Same as Fig. 1, but for the hydroxyl-covered PbO-terminated (001) slab. The zero of energy in the LaDOS plots coincides with the Fermi level

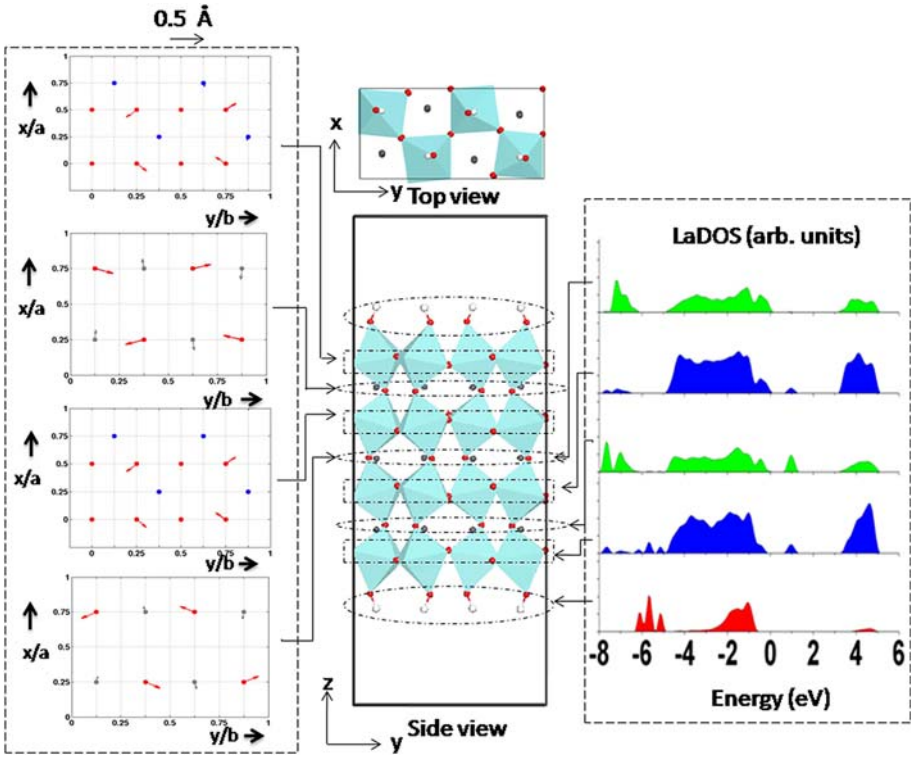

Fig. 5 Same as Fig. 4, but for the hydroxyl-covered ZrO_2-terminated (001) slab

in most cases studied here indicates that stable PZ nanoparticles in the A_O phase can be synthesized, as experimentally shown by some of us (Tan DQ et al., unpublished manuscript).

Summary

Our ab initio study of the three bulk phases of $PbZrO_3$ has shown that the orthorhombic antiferroelectric phase is the ground state, with the rhombohedral ferroelectric and cubic paraelectric phases being 0.14 and 0.39 eV per formula unit higher in energy, respectively.

In the case of the PbO-terminated clean (001) surface, the nature of the antiferroelectric distortions in the surface regions are almost identical to that in bulk $PbZrO_3$, and show a fast convergence to bulk behavior as one moves inward. In contrast, the clean ZrO_2-terminated (001) surface favors antiferroelectric distortions which differ significantly from the bulk-like patterns and show a relatively slow convergence to bulk behavior. However, in both of these cases, the electronic structure in the surface region is identical to that of the bulk, with the prominent absence of surface states.

Hydroxyl-covered surfaces, intended to model excessively oxidized (001) surfaces, display markedly different behavior. The hydroxyl-covered PbO-terminated surface displays large out-of-layer displacements of surface Pb atoms with the hydroxyl group preferring bridge sites between adjacent Pb atoms. In case of the ZrO_2-terminated surface, the hydroxyl group relaxes to complete the ZrO_6 octahedron on the surface. In both cases, the polarization patterns in the surface region are qualitatively different from the corresponding ones in bulk. Consistent with the significant atomic rearrangement in the surface regions of both these cases, surface states can be seen in the band gap region, as evidenced by our density of states analysis, indicating that these excessively oxidized surfaces could be metallic.

Acknowledgements GP and RR would like to acknowledge financial support of this work by a grant from DARPA through a subcontract from General Electric. Helpful discussions with Dr. Steve Boggs and Dr. Pamir Alpay are gratefully acknowledged.

References

1. Scott JF (2007) Science 315:954
2. Watton R (1989) Ferroelectrics 91:87
3. Whatmore RW (1991) Ferroelectrics 118:241
4. Lines ME, Glass AM (1977) Principles and applications of ferroelectric and related materials. Clarendon, Oxford
5. Noguera C (1996) Physics and chemistry at oxide surfaces. Cambridge University Press, New York
6. Jona F, Shirane G, Mazzi F, Pepinsky R (1957) Phys Rev 105:849
7. Whatmore RW, Glazer AM (1979) J Phys C 12:1505
8. Sawaguchi E, Shiozaki Y, Fujishita H, Tanaka M (1980) J Phys Soc Jpn 49(suppl B):191

9. Fujishita H, Shiozaki Y, Achiwa N, Sawaguchi E (1982) J Phys Soc Jpn 51:3583
10. Tanaka M, Saito R, Tsuzuki K (1982) J Phys Soc Jpn 51:2635
11. Fujishita H, Hoshino S (1984) J Phys Soc Jpn 53:226
12. Fujishita H, Katano S (2000) Ferroelectrics 237:209
13. Fujishita H, Tanaka S (2001) Ferroelectrics 258:37
14. Fujishita H, Ishikawa Y, Tanaka S, Ogawaguchi A, Katano S (2003) J Phys Soc Jpn 72:1426
15. Singh DJ (1995) Phys Rev B 52:12559
16. Johannes MD, Singh DJ (2005) Phys Rev B 71:212101
17. Robertson J (2000) J Vac Sci Technol B 18(3):1785
18. Piskunov S, Gopeyenko A, Kotomin EA, Zhukovskii YuF, Ellis DE (2007) Comput Mater Sci 41:195
19. Kresse G, Furthmuller J (1996) Phys Rev B 54:11169
20. Monkhorst HJ, Pack JD (1976) Phys Rev B 13(12):5188
21. Aoyagi S, Kuroiwa Y, Sawada A, Tanaka H, Harada J, Nishibori E, Takata M, Sakata M (2002) J Phys Soc Jpn 71:2353
22. Kagimura R, Singh DJ (2008) Phys Rev B 77:104113
23. Baedi J, Hosseini SM, Kompany A, Attaran Kakhki E (2008) Phys Status Solidi (B) 245:2572
24. Leung K, Wright AF (2002) Ferroelectrics 281:171
25. Eglitis RI, Vanderbilt D (2007) Phys Rev B 76:155439